Pressure-enhanced robustness of helical edge state in ABA Tri-layer Graphene

Shijie Fang[1], Hua Fan[2], Jifeng Shao[1], and Yue Zhao[1,2,3]*
1 Shenzhen Institute for Quantum Science and Engineering (SIQSE), Southern University of Science and Technology (SUSTech), China
2 Department of Physics, SUSTech, China and
3 International Quantum Academy, Shenzhen, Guangdong 518048, China

Multi-layer graphene systems are promising platforms to study interesting physical phenomena, including unique quantum hall physics, spontaneous symmetry breaking, and topological properties. Here, by applying hydrostatic pressure on the tri-layer ABA graphene, the phase diagram at the charge neutrality point undergoes a significant change, indicating a complicated interplay among different energy scales. Also, quantum parity hall state, a kind of helical edge state protected by mirror symmetry, emerges after pressure. The measured Landau Fan diagram illustrates the modification of the band structure by pressure, which can be used to explain the observed phenomenon.

INTRODUCTION

Regarding multilayer graphene systems, their rich physical properties make them widely regarded as a platform for studying unconventional properties of two-dimensional electron systems. Up to now, many intriguing physical phenomena has been found in multilayer graphene systems, ranging from single-particle to many-body physics, such as the Lifshitz transition of Fermi surface topology [1, 2], Landau level physics in the single-particle picture [3–6], quantum hall ferromagnetism even fractionalization under a high perpendicular magnetic field [7–17], and various symmetry broken states near charge neutrality and under a relatively small magnetic field [18–21]. Besides these phenomena, insulating bulk states with non-trivial edge channels can emerge in various graphene systems under different conditions, including chiral and helical edge states [19, 22–29].

Among them, tri-layer ABA graphene has attracted widespread attention due to its unique band structure at low energy regime. As a highly tunable platform, it provides an excellent opportunity to study its single-particle band structure and many-body phenomenon. In previous studies, its electronic properties have been studied by tuning multiple control knobs like carrier density, displacement field, and magnetic field, which lead to many interesting discoveries in this system [2–6, 15–17, 19, 20]. Notably, because the low-energy band structure of multilayer graphene is highly sensitive to the interlayer hopping strength, applying hydrostatic pressure to reduce the interlayer distance and further study its properties has become a highly promising research approach.

In recent years, condensed matter physics has witnessed a growing interest in exploring the topologically non-trivial edge states in materials. As an extension of the chiral edge state, the helical edge state is a special boundary state featured by the non-dissipative channels with opposite motion directions. Helical conductors have been proposed to realize Majorana statistics for quantum computation [30–33]. Since its first theoretical proposed [34, 35], multiple ways are developed to achieve helical edge states, including topologically non-trivial band structures protected by time-reversal symmetry, such as those found in QSHE systems [36, 37]. In addition, in those systems where the conduction band is energetically below the valence band, the introduction of a magnetic field can cause the crossing of "hole-like" Landau levels with "electron-like" Landau levels at the system's boundary, leading to the emergence of spin-degenerate helical edge states which are composed of opposite-propagating chiral edge states. The advent of multilayer graphenes has provided a fertile platform for exploring different types of helical edge states because of the unique band structure near the charge neutrality point (CNP). Many experimental evidence has confirmed the existence of helical edge states in multilayer graphene systems, ranging from monolayer to tetralayer graphene [19, 23, 24, 26, 38].

Here we report the dramatic change of phase diagram at the charge neutrality point and the emergence of a kind of helical edge state, named quantum parity hall effect, after applying 1.0 GPa hydrostatic pressure. Tri-layer ABA graphene is one of the material platforms which can hold helical edge states owing to its unique band structure. The low-energy band structure of tri-layer ABA graphene consists of a monolayer-like valence band and a bilayer-like conduction band in the absence of displacement field, which have an energy overlap, as shown in Figure 1(b). Both branches are protected by mirror symmetry and have odd(monolayer) or even(bilayer) parity. However, when a displacement field is applied, they mix due to the breaking of mirror symmetry.

METHOD AND CHARACTERIZATION

Here, we fabricate the tri-layer ABA device that has high mobility for observing its quantum hall effect, and we changed its band structure and phase diagram by exerting hydrostatic pressure out of the plane. Our device

* Author1 e-mail

is a high-quality dual-gate device with a Hall-bar geometry, with hexagonal boron nitride(h-BN) as the dielectric spacer and few-layer graphite as the top and bottom gates, which is stacked together using a dry-transfer method [39]. In detail, the tri-layer ABA graphene is encapsulated by two hBN sheets whose geometric capacitances are C_t, C_b, respectively, in the unit of $V^{-1}cm^{-2}$. Moreover, outside of hBN sheets, two graphite stacks act as top and bottom gates. By modulating the top gate voltage V_t and bottom-gate voltage V_b, the carrier density $n(10^{12}cm^{-2})$ and out-of-plane displacement field $D(V/nm)$ can be tuned continuously, according to the relation:

$$n = C_tV_t + C_bV_b, D = \frac{1}{2\epsilon_0}(C_tV_t - C_bV_b)$$

with ϵ_0 the vacuum permittivity. So, this configuration enables us to measure its transport properties with multiple in-situ tunable external parameters.

We also utilized hydrostatic pressure to reduce the interlayer distance and strengthen the interlayer coupling. It can change the material structure of Van der Waals(VdW) material systems without enhanced disorder effect, thanks to their weak out-of-plane VdW bonding. Previous work shows that hydrostatic pressure can compress the interlayer distance of graphene superlattice by 5% with less than 2.5 GPa[40] and can induce superconductivity in twisted bilayer graphene away from magic angle[41]. Therefore, hydrostatic pressure is a powerful tool for tuning the electronic structure effectively. Here, we mainly investigate the change of the device under a 1.0 GPa hydrostatic pressure by comparing it to that in ambient pressure.

The high quality of this device can be verified by the dependence of longitudinal resistance as a function of n and D. An external out-of-plane displacement field opens a gap at the charge neutrality point, schematically shown in Fig. 1(b). Fig. 1(c) and (d) show the resistance of the device at zero magnetic fields before and after pressurization. It is found that, along the charge neutrality point, the resistance of both increases dramatically, which indicates the appearance of an electric-field-induced band gap. This signature reflects a good quality and low disorder of our device before and after pressurization, which enables us to study the sample's band structure using the Landau fan diagram under an out-of-plane magnetic field.

In this work, transport measurements were conducted on this tri-layer ABA graphene device before and after 1.0 GPa pressure at a temperature T = 1.6K, and our findings are three-fold. Firstly, we explore the phase diagram of the tri-layer ABA graphene at the charge neutrality point as a function of the magnetic field and displacement field, by making a slow scan of the displacement field around and magnetic field around. The one after pressure reveals a complex competition between different energy scales. Interestingly, we observe the signatures of some helical edge state after pressure, indicated by its nearly quantized four-terminal longitudinal conductance and near-zero transverse resistance. This state fades away when D is large enough, demonstrating that it is protected by mirror symmetry, which is broken under a finite D field. Secondly, in order to partially explain the observed phenomenon above, we perform the magneto-transport measurement to investigate how the pressure modifies the hopping parameters. Specifically, the Landau fan diagram shows that the crossing points among Landau levels undergo a significant shift, appearing at a larger magnetic field at 1.0 GPa pressure. This phenomenon indicates that the strength of interlayer hopping, alternatively, the low energy band structure, can be modified by pressure. Finally, our magneto-transport measurement finds some signatures of the four-fold quasi-degenerate zeroth monolayer-like Landau levels, which cannot be explained under the single-particle picture. These signatures include the complete splitting of these degenerate Landau levels at a relatively high magnetic field (10 T) before and after pressure. Besides, we found the Landau level splitting at the intermediate magnetic field only after pressurization. These two signatures indicate that the enlarged Landau level gaps, which are inconsistent with the single particle picture, should be associated with enhancing interlayer exchange interaction.

RESULTS

CONCLUSION

In conclusion, this work reveals the highly tunable properties in tri-layer ABA graphene by hydrostatic pressure. It is seen that not only the hopping parameters can be tuned by pressure directly, but the phase diagram in the low magnetic field can also have a significant change. These phenomena demonstrate that tri-layer ABA graphene can be a high-tunable platform for band engineering and a variety of phases with pressurization. It is the emergence of the "Quantum Parity Hall state," which is a helical edge state with two pairs of counter-propagating edge modes. Moreover, several novel states are favoured by different energy scales at the charge neutrality point. However, there are still some questions which still need to be answered. The first one is about what the nature of the phase B. In order to answer it, it is necessary to use the temperature-varied and tilted magnetic field transport measurement to get a more detailed understanding of the competition between different energy scales. Since the perpendicular magnetic field controls the exchange effects and the LL degeneracies, they may play an important role in determining the phase

diagram, revealing the complex Landau-level structure of tri-layer ABA graphene. We hope our experimental results can trigger some theoretical and experimental interests to investigate it deeper.

ACKNOWLEGEMENT

Coming Soon !

[1] Y. Shi, S. Che, K. Zhou, S. Ge, Z. Pi, T. Espiritu, T. Taniguchi, K. Watanabe, Y. Barlas, R. Lake, *et al.*, Tunable lifshitz transitions and multiband transport in tetralayer graphene, Physical review letters **120**, 096802 (2018).

[2] W. Bao, L. Jing, J. Velasco Jr, Y. Lee, G. Liu, D. Tran, B. Standley, M. Aykol, S. Cronin, D. Smirnov, *et al.*, Stacking-dependent band gap and quantum transport in trilayer graphene, Nature Physics **7**, 948 (2011).

[3] T. Taychatanapat, K. Watanabe, T. Taniguchi, and P. Jarillo-Herrero, Quantum hall effect and landau-level crossing of dirac fermions in trilayer graphene, Nature Physics **7**, 621 (2011).

[4] L. C. Campos, T. Taychatanapat, M. Serbyn, K. Surakitbovorn, K. Watanabe, T. Taniguchi, D. A. Abanin, and P. Jarillo-Herrero, Landau level splittings, phase transitions, and nonuniform charge distribution in trilayer graphene, Physical Review Letters **117**, 066601 (2016).

[5] S. Che, P. Stepanov, S. Ge, M. Zhu, D. Wang, Y. Lee, K. Myhro, Y. Shi, R. Chen, Z. Pi, *et al.*, Substrate-dependent band structures in trilayer graphene/h- bn heterostructures, Physical Review Letters **125**, 246401 (2020).

[6] Y. Shimazaki, T. Yoshizawa, I. V. Borzenets, K. Wang, X. Liu, K. Watanabe, T. Taniguchi, P. Kim, M. Yamamoto, and S. Tarucha, Landau level evolution driven by band hybridization in mirror symmetry broken aba-stacked trilayer graphene, arXiv preprint arXiv:1611.02395 (2016).

[7] F. Zhang, D. Tilahun, and A. H. MacDonald, Hund's rules for the n= 0 landau levels of trilayer graphene, Physical Review B **85**, 165139 (2012).

[8] A. F. Young, C. R. Dean, L. Wang, H. Ren, P. Cadden-Zimansky, K. Watanabe, T. Taniguchi, J. Hone, K. L. Shepard, and P. Kim, Spin and valley quantum hall ferromagnetism in graphene, Nature Physics **8**, 550 (2012).

[9] X. Liu, G. Farahi, C.-L. Chiu, Z. Papic, K. Watanabe, T. Taniguchi, M. P. Zaletel, and A. Yazdani, Visualizing broken symmetry and topological defects in a quantum hall ferromagnet, Science **375**, 321 (2022).

[10] A. Coissard, D. Wander, H. Vignaud, A. G. Grushin, C. Repellin, K. Watanabe, T. Taniguchi, F. Gay, C. B. Winkelmann, H. Courtois, *et al.*, Imaging tunable quantum hall broken-symmetry orders in graphene, Nature **605**, 51 (2022).

[11] B. Hunt, J. D. Sanchez-Yamagishi, A. F. Young, M. Yankowitz, B. J. LeRoy, K. Watanabe, T. Taniguchi, P. Moon, M. Koshino, P. Jarillo-Herrero, *et al.*, Massive dirac fermions and hofstadter butterfly in a van der waals heterostructure, Science **340**, 1427 (2013).

[12] G. Yu, R. Gorbachev, J. Tu, A. Kretinin, Y. Cao, R. Jalil, F. Withers, L. Ponomarenko, B. Piot, M. Potemski, *et al.*, Hierarchy of hofstadter states and replica quantum hall ferromagnetism in graphene superlattices, Nature physics **10**, 525 (2014).

[13] B. Hunt, J. Li, A. Zibrov, L. Wang, T. Taniguchi, K. Watanabe, J. Hone, C. Dean, M. Zaletel, R. Ashoori, *et al.*, Direct measurement of discrete valley and orbital quantum numbers in bilayer graphene, Nature communications **8**, 948 (2017).

[14] K. Lee, B. Fallahazad, J. Xue, D. C. Dillen, K. Kim, T. Taniguchi, K. Watanabe, and E. Tutuc, Chemical potential and quantum hall ferromagnetism in bilayer graphene, Science **345**, 58 (2014).

[15] Y. Lee, J. Velasco Jr, D. Tran, F. Zhang, W. Bao, L. Jing, K. Myhro, D. Smirnov, and C. N. Lau, Broken symmetry quantum hall states in dual-gated aba trilayer graphene, Nano letters **13**, 1627 (2013).

[16] P. Stepanov, Y. Barlas, T. Espiritu, S. Che, K. Watanabe, T. Taniguchi, D. Smirnov, and C. N. Lau, Tunable symmetries of integer and fractional quantum hall phases in heterostructures with multiple dirac bands, Physical review letters **117**, 076807 (2016).

[17] B. Datta, S. Dey, A. Samanta, H. Agarwal, A. Borah, K. Watanabe, T. Taniguchi, R. Sensarma, and M. M. Deshmukh, Strong electronic interaction and multiple quantum hall ferromagnetic phases in trilayer graphene, Nature communications **8**, 14518 (2017).

[18] R. T. Weitz, M. T. Allen, B. E. Feldman, J. Martin, and A. Yacoby, Broken-symmetry states in doubly gated suspended bilayer graphene, Science **330**, 812 (2010).

[19] P. Stepanov, Y. Barlas, S. Che, K. Myhro, G. Voigt, Z. Pi, K. Watanabe, T. Taniguchi, D. Smirnov, F. Zhang, *et al.*, Quantum parity hall effect in bernal-stacked trilayer graphene, Proceedings of the National Academy of Sciences **116**, 10286 (2019).

[20] A. A. Zibrov, P. Rao, C. Kometter, E. M. Spanton, J. Li, C. R. Dean, T. Taniguchi, K. Watanabe, M. Serbyn, and A. F. Young, Emergent dirac gullies and gully-symmetry-breaking quantum hall states in a b a trilayer graphene, Physical Review Letters **121**, 167601 (2018).

[21] F. Winterer, A. M. Seiler, A. Ghazaryan, F. R. Geisenhof, K. Watanabe, T. Taniguchi, M. Serbyn, and R. T. Weitz, Spontaneous gully-polarized quantum hall states in aba trilayer graphene, Nano Letters **22**, 3317 (2022).

[22] F. Zhang, J. Jung, G. A. Fiete, Q. Niu, and A. H. MacDonald, Spontaneous quantum hall states in chirally stacked few-layer graphene systems, Physical review letters **106**, 156801 (2011).

[23] A. Young, J. Sanchez-Yamagishi, B. Hunt, S. Choi, K. Watanabe, T. Taniguchi, R. Ashoori, and P. Jarillo-Herrero, Tunable symmetry breaking and helical edge transport in a graphene quantum spin hall state, Nature **505**, 528 (2014).

[24] L. Veyrat, C. Déprez, A. Coissard, X. Li, F. Gay, K. Watanabe, T. Taniguchi, Z. Han, B. A. Piot, H. Sellier, *et al.*, Helical quantum hall phase in graphene on srtio3, Science **367**, 781 (2020).

[25] F. R. Geisenhof, F. Winterer, A. M. Seiler, J. Lenz, T. Xu, F. Zhang, and R. T. Weitz, Quantum anoma-

lous hall octet driven by orbital magnetism in bilayer graphene, Nature **598**, 53 (2021).
[26] P. Maher, C. R. Dean, A. F. Young, T. Taniguchi, K. Watanabe, K. L. Shepard, J. Hone, and P. Kim, Evidence for a spin phase transition at charge neutrality in bilayer graphene, Nature Physics **9**, 154 (2013).
[27] E. M. Spanton, A. A. Zibrov, H. Zhou, T. Taniguchi, K. Watanabe, M. P. Zaletel, and A. F. Young, Observation of fractional chern insulators in a van der waals heterostructure, Science **360**, 62 (2018).
[28] F. Winterer, F. R. Geisenhof, N. Fernandez, A. M. Seiler, F. Zhang, and R. T. Weitz, Ferroelectric and anomalous quantum hall states in bare rhombohedral trilayer graphene, arXiv preprint arXiv:2305.04950 (2023).
[29] T. Han, Z. Lu, G. Scuri, J. Sung, J. Wang, T. Han, K. Watanabe, T. Taniguchi, H. Park, and L. Ju, Correlated insulator and chern insulators in pentalayer rhombohedral stacked graphene, arXiv preprint arXiv:2305.03151 (2023).
[30] X.-L. Qi and S.-C. Zhang, Topological insulators and superconductors, Reviews of Modern Physics **83**, 1057 (2011).
[31] M. Z. Hasan and C. L. Kane, Colloquium: topological insulators, Reviews of modern physics **82**, 3045 (2010).
[32] Y. Oreg, G. Refael, and F. Von Oppen, Helical liquids and majorana bound states in quantum wires, Physical review letters **105**, 177002 (2010).
[33] R. M. Lutchyn, J. D. Sau, and S. D. Sarma, Majorana fermions and a topological phase transition in semiconductor-superconductor heterostructures, Physical review letters **105**, 077001 (2010).
[34] C. L. Kane and E. J. Mele, Quantum spin hall effect in graphene, Physical review letters **95**, 226801 (2005).
[35] C. L. Kane and E. J. Mele, Z 2 topological order and the quantum spin hall effect, Physical review letters **95**, 146802 (2005).
[36] B. A. Bernevig, T. L. Hughes, and S.-C. Zhang, Quantum spin hall effect and topological phase transition in hgte quantum wells, science **314**, 1757 (2006).
[37] A. Roth, C. Brüne, H. Buhmann, L. W. Molenkamp, J. Maciejko, X.-L. Qi, and S.-C. Zhang, Nonlocal transport in the quantum spin hall state, Science **325**, 294 (2009).
[38] S. Che, Y. Shi, J. Yang, H. Tian, R. Chen, T. Taniguchi, K. Watanabe, D. Smirnov, C. N. Lau, E. Shimshoni, *et al.*, Helical edge states and quantum phase transitions in tetralayer graphene, Physical Review Letters **125**, 036803 (2020).
[39] L. Wang, I. Meric, P. Huang, Q. Gao, Y. Gao, H. Tran, T. Taniguchi, K. Watanabe, L. Campos, D. Muller, *et al.*, One-dimensional electrical contact to a two-dimensional material, Science **342**, 614 (2013).
[40] M. Yankowitz, J. Jung, E. Laksono, N. Leconte, B. L. Chittari, K. Watanabe, T. Taniguchi, S. Adam, D. Graf, and C. R. Dean, Dynamic band-structure tuning of graphene moiré superlattices with pressure, Nature **557**, 404 (2018).
[41] M. Yankowitz, S. Chen, H. Polshyn, Y. Zhang, K. Watanabe, T. Taniguchi, D. Graf, A. F. Young, and C. R. Dean, Tuning superconductivity in twisted bilayer graphene, Science **363**, 1059 (2019).

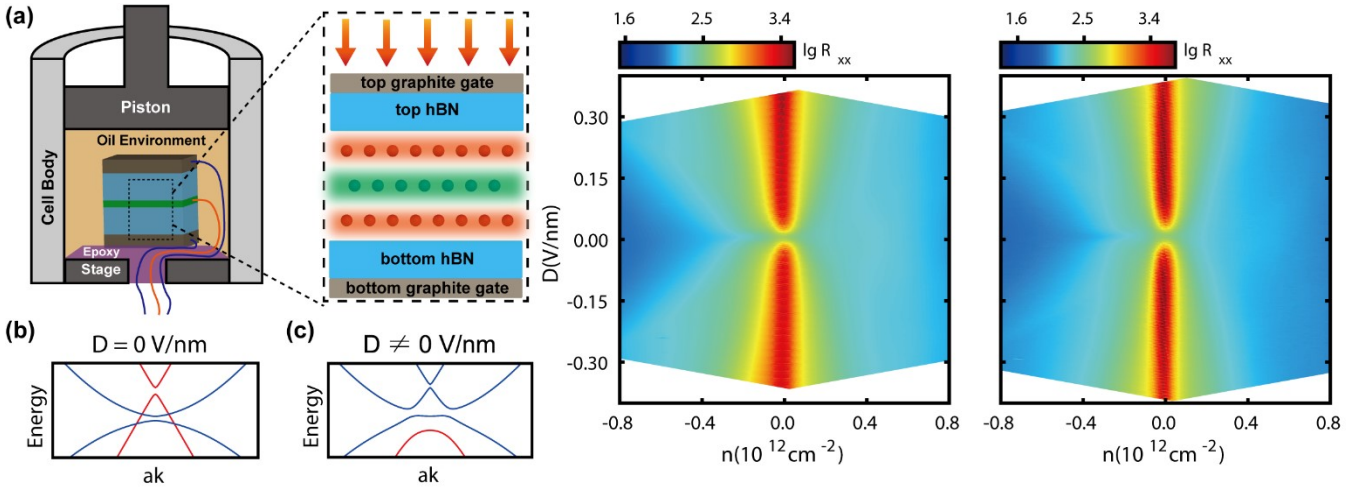

FIG. 1. Schematic of experimental setup and transport characterization.
(a) Schematics of hydrostatic pressure setup. (b), (c) Schematics of How the displacement field influences the band structure of tri-layer ABA graphene. In the absence of displacement field D, the low energy bands include two monolayer-like bands with linear dispersion (red curve & blue curve) and two bilayer-like bands with parabolic dispersion (cyan curve & green curve). When D is non-zero, these two bands hybridize, leading to a gap opening at the charge neutrality point, making the system insulate. (d), (e) device characterization before and after 1.0 GPa hydrostatic pressure by using the four-terminal longitudinal resistance R_{xx} as a function of carrier density $n(10^{12}cm^{-2})$ and displacement field D(V/nm). Along the charge neutrality profile, the resistance increases dramatically as D increases, indicating a gap opening reflecting the device's good quality.

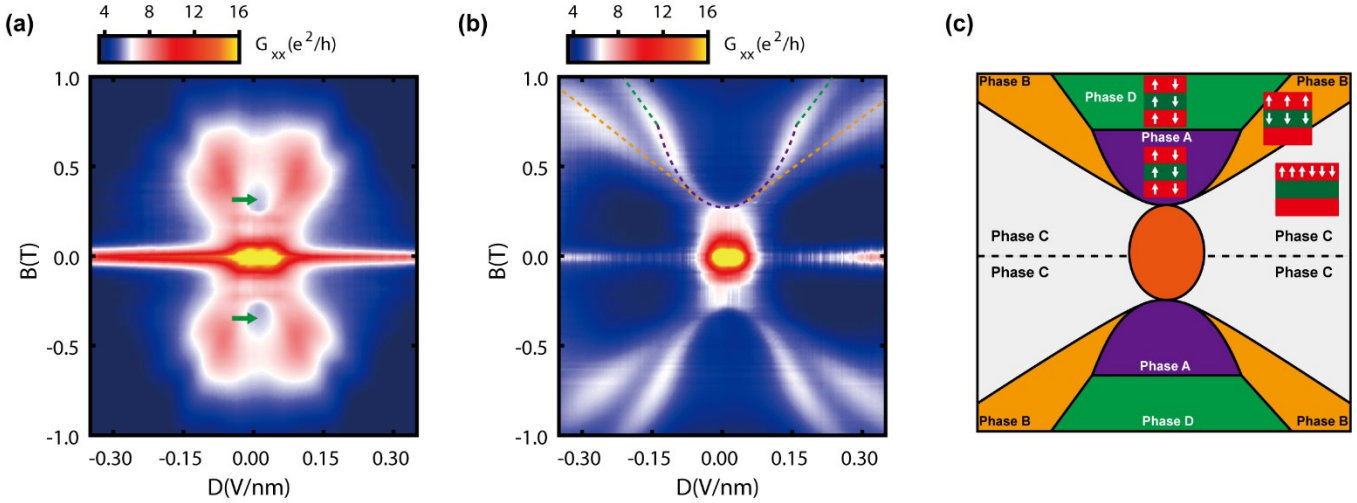

FIG. 2. Phase diagrams at the charge neutrality point before and after 1.0 GPa hydrostatic pressure.
Here, Figures 2(a) and 2(b) show the phase diagrams of four-terminal longitudinal conductance G_{xx} in unit of $\frac{e^2}{h}$ as a function of B(T) and D(V/nm), with B ranges from -1.0 T to 1.0 T and D ranges from -0.30 V/nm to 0.30 V/nm, it is noted that the values larger than 16 has been rescaled to 16. (a) shows the phase diagram at 0 GPa. A prominent feature emerges around D = 0 V/nm and B = 0.3T, indicated by the green arrow. (b) the phase diagram at 1GPa shows visible traces of phase boundary (marked by dashed lines of different colours), indicating first-order phase transitions between different ground states. This phase diagram is converted into a cartoon shown in (c). Different regions are filled with different colours, and specific phases are labelled with A, B, and C, demonstrating the existence of different ground states.

TABLE I. This is a table that records the fitting parameters at 0 Gpa and 1 Gpa based on the experimental results shown in figure.4(a)(b), the energy unit is set to eV. The intralayer hopping γ_0 is fixed as $3.100eV$.

Pressure	γ_0	γ_1	γ_2	γ_3	γ_4	γ_5	δ	Δ_2
0 GPa	3.100	0.3845	−0.0194	0.3510	0.0653	0.0636	0.0415	0.0021
1 GPa	3.100	0.3784	−0.0234	0.3665	0.0612	0.0833	0.0534	0.0031

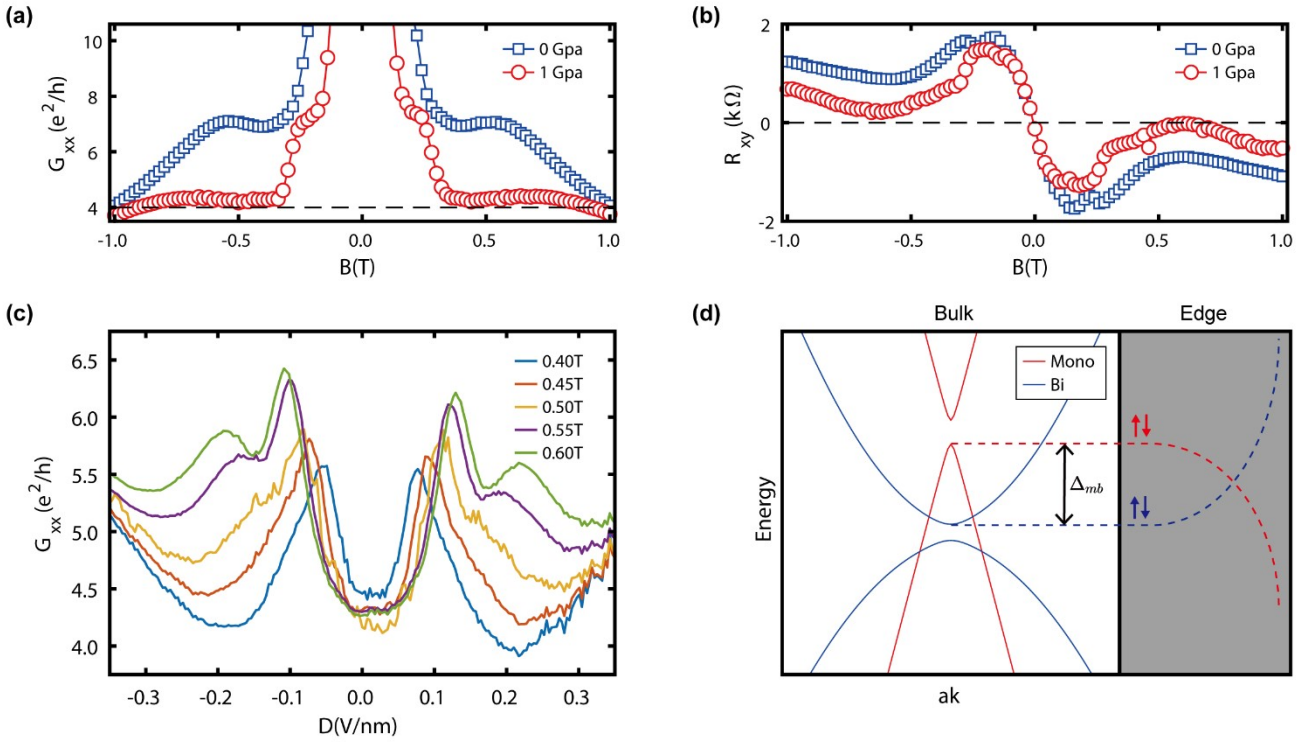

FIG. 3. Experimental signatures of Quantum Parity Hall effect and its schematics.
(a) The longitudinal conductance G_{xx} profiles of the D = 0 V/nm in both Figure 2(a) and 2(b), blue squares mark the 0 GPa curve, and red circles mark the 1 GPa curve. It can be seen that G_{xx} becomes nearly quantized (about $4.1\frac{e^2}{h}$) after pressure. (b) The profiles of transverse resistance R_{xx} at D = 0 V/nm, where the 1 GPa curve almost reaches zero around B = 0.6T, together with the nearly quantized signature in (a), indicating the appearance of helical edge states in the system, which is the quantum parity hall state (QPHE). (c) The profiles at B = 0.40 / 0.45 / 0.50 / 0.55 / 0.60 T are taken from Figure 2(b) as a function of displacement field D. The nearly quantized plateau disappears when D is large enough. (d) The schematic of the mechanism of (QPHE) based on the band structure: the edge states from the monolayer valence band and that from the bilayer conduction band propagate along opposite directions along the edge, and because of the spin degeneracy, there are four channels of edge states.

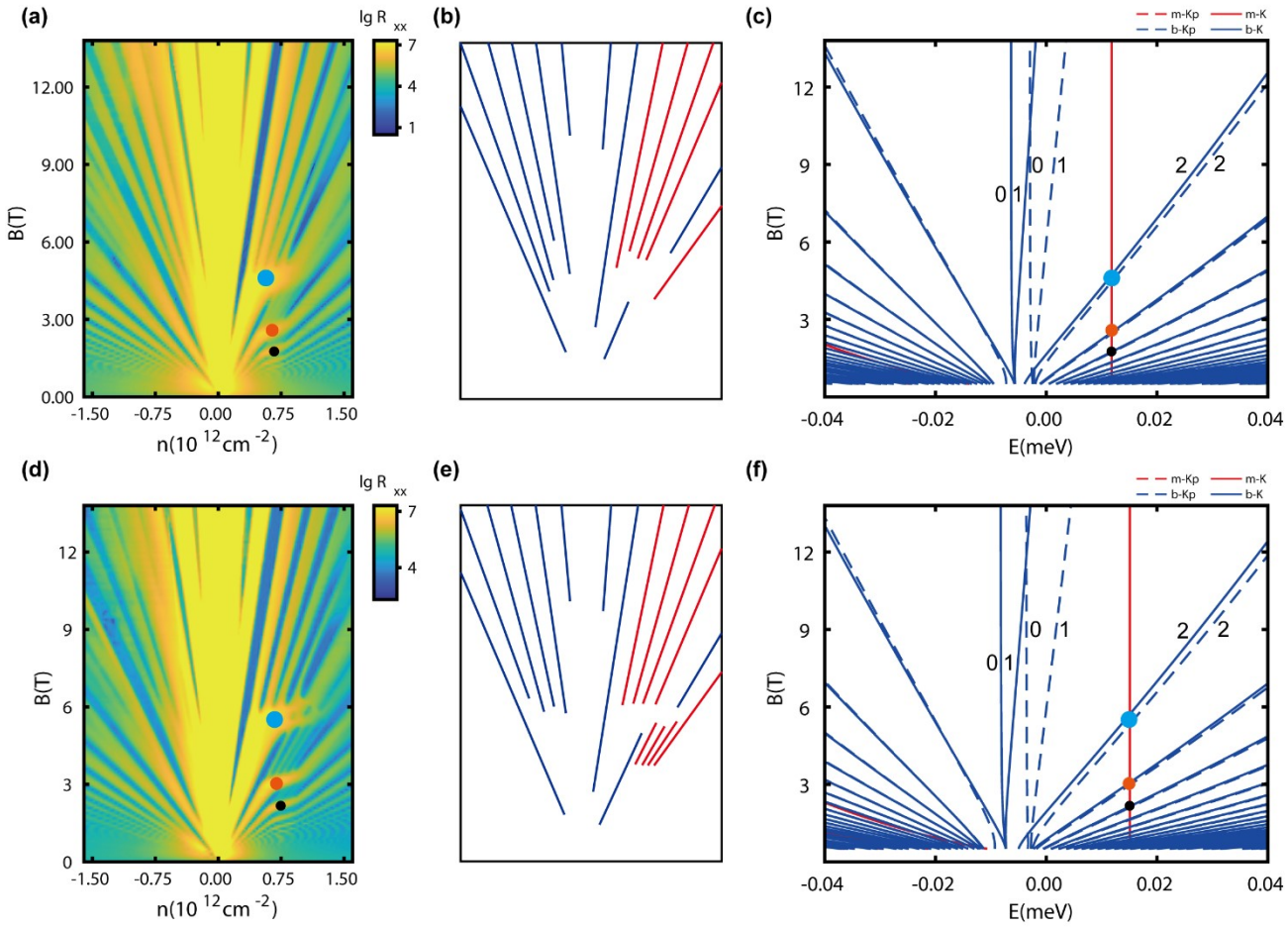

FIG. 4. Landau Fan diagrams at 0 GPa and 1 GPa, and the fitted simulation results.
(a), (d) the Landau Fan diagrams at 0 GPa and 1 GPa, the crossing points between $(m, K/K', 0)$ and $(b, K', 2), (b, K', 3), (b, K', 4)$ are marked by cyan, orange and black-coloured dots (P1, P2 and P3). It can be seen that the crossing points shift toward a large magnetic field after pressure. In (b) (e), some minimum tracks at low integer fillings (from -6 to 10) are traced out, the blue colour indicates that the LLs are from a bilayer-like branch while the red is from monolayer-like branch. (c), (f) the simulated Landau level structures fitted by the positions of crossing points from (a) and (b). The corresponding points are also marked in the figures. The monolayer-like Landau levels are red-color, while the bilayer-like Landau levels are blue-colour (dashed line for K' valley and solid line for K valley). The numbers are the Landau level indexes in each branch. The fitting parameters are listed in Table I.